

## **CO<sub>2</sub> Absorption Rate and Solubility in Monoethanolamine/Piperazine/Water**

Hongyi Dang (dang@che.utexas.edu)  
Gary T. Rochelle\* ([gtr@che.utexas.edu](mailto:gtr@che.utexas.edu), 512-471-7230)  
*The University of Texas at Austin*  
*Department of Chemical Engineering*  
*Austin, Texas 78712*

*Prepared for presentation at the First National Conference on Carbon Sequestration,  
Washington, DC, May 14-17, 2001*

### **ABSTRACT**

The solubility and absorption rate of carbon dioxide into monoethanolamine/ piperazine/water were measured in a wetted wall column at 40-60°C. The total amine concentration was varied from 1.0 M to 5.0 M with monoethanolamine blends containing 0 to 1.2 M piperazine. CO<sub>2</sub> solubility and solution speciation were simulated by nine equilibrium reactions. Two of the equilibrium constants were adjusted to match literature data. The rate of absorption was predicted by the theory of diffusion with fast chemical reaction. Piperazine at 24 mol% of the total amine decreases CO<sub>2</sub> equilibrium pressure by 50% and enhances CO<sub>2</sub> absorption rate by 50% to 100%. The CO<sub>2</sub> enhancement factor decreases by an order of magnitude as loading increases from 0 to 0.5 moles CO<sub>2</sub>/mole amine.

\*Author to whom correspondence should be addressed

### **INTRODUCTION**

Aqueous monoethanolamine (MEA) is widely used for removing carbon dioxide (CO<sub>2</sub>) from natural gas streams and refinery process streams. It is also used to remove CO<sub>2</sub> from combustion gases and may receive wide application for abatement of greenhouse gases. MEA is a relative strong base with a fast reaction rate, yielding a low CO<sub>2</sub> concentration. A number of investigators have studied the solubility (12, 15, 16, 23) and reaction kinetics (1, 7, 9, 11, 14) of CO<sub>2</sub> in aqueous MEA.

Even though MEA reacts relatively fast with CO<sub>2</sub>, the rate of absorption is still controlled by reaction kinetics. Typical absorber tray efficiency is less than 20%. Piperazine (PZ) has been studied as a promoter for methyldiethanolamine (MDEA) by Xu et al. (26, 27, 28) and Kaganoi (13). Bishnoi (5) has determined that the rate constant of PZ with CO<sub>2</sub> is one order of magnitude higher than that of MEA with CO<sub>2</sub>. Therefore a blend of MEA and PZ should absorb CO<sub>2</sub> faster than MEA alone.

The objective of this work is to quantify the effectiveness of PZ as a rate promoter in aqueous MEA. The solubility and absorption rate of CO<sub>2</sub> in MEA/PZ/H<sub>2</sub>O have been measured in loaded and lean solutions with a wetted wall column. The results are compared with the predictions of a simple vapor-liquid equilibrium model and a simple rate model.

## EXPERIMENTAL APPARATUS AND METHODS

The wetted wall column (Figure 1) was constructed from a stainless steel tube with a well defined surface area ( $38.52 \text{ cm}^2$ ) and a characteristic liquid film mass transfer coefficient similar to that of a packed tower. The stainless steel tube was 9.1 cm long and had an outside diameter of 1.26 cm. Liquid overflowed from the inside and formed a liquid film over the outer surface of the stainless steel tube. Gas entered the wetted wall column from the bottom and countercurrently contacted the liquid film. Figure 2 shows the overall flow diagram of the apparatus used in this study to obtain solubility and absorption rate data. The apparatus was originally built by Mshewa (19) and modifications were made by Pacheco et al. (20, 21). More details are given by Dang (8).

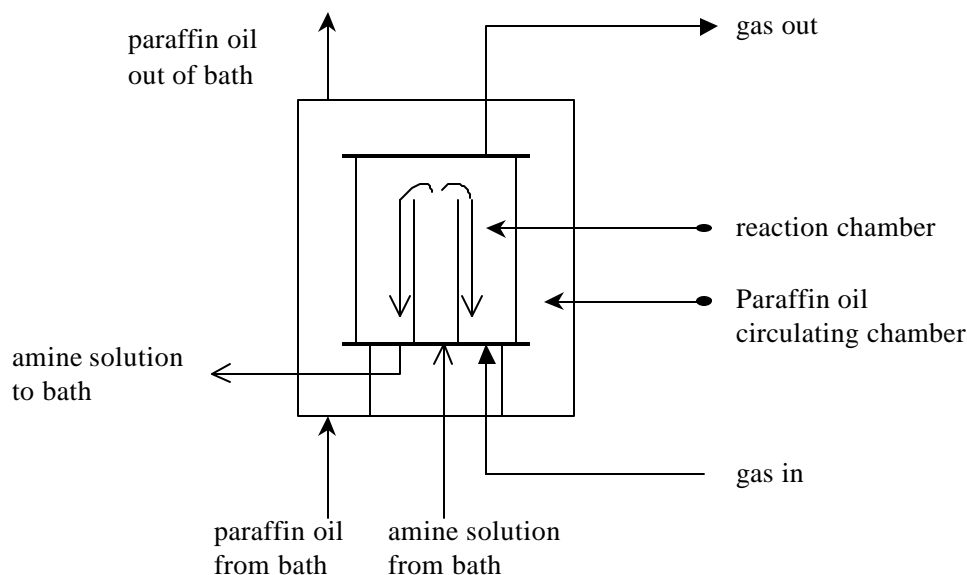


Figure 1. Detailed column diagram.

Flow from two gas cylinders was regulated by Brooks model 5850E mass flow controllers. The gas was presaturated at the same temperature as the wetted wall column. The total pressure used in this work was around 4 to 5 atm. To minimize gas film resistance, the gas flow rate was approximately 5 to 6 SLPM.

The gas was sent from the column through a needle valve where the pressure was reduced to atmospheric. From the downstream side of the needle valve, the gas was sent to a condenser that consisted of an Erlenmeyer flask submerged in ice water. The gas was then passed on to a series of Horiba PIR 2000 carbon dioxide analyzers where the outlet carbon dioxide concentration was measured by infrared spectroscopy. Two analyzers were used, each having a different concentration range (0-25% and 0-0.25%, volume basis).

The amine solution was kept in a reservoir and passed through a coil submerged in an oil bath to heat it to the reactor temperature. Anhydrous piperazine (99.9%) from Aldrich Chemical and MEA from a commercial supplier were mixed with de-ionized water to make up the amine solution. The flow of amine solution was provided by a Cole-Parmer micropump and was measured by a liquid rotameter. The liquid flow rate was  $3 \text{ cm}^3/\text{s}$ . A reservoir with a  $400 \text{ cm}^3$

holdup was used for the amine solution. The paraffin oil in the bath was also circulated to the wetted wall column, keeping the entire apparatus at a uniform temperature. The inlet and outlet temperatures of the amine solution were measured, which have a difference of 1 to 2°C and the temperature in the column was approximated by the average of the inlet and outlet temperatures.

Absorption or desorption of CO<sub>2</sub> was determined from the gas phase material balance using the measured inlet and outlet gas concentrations. Periodically, liquid samples were withdrawn from a sample port close to the reactor outlet and analyzed for total carbon dioxide by acidic evolution into a CO<sub>2</sub> analyzer (6, 13, 19, 20, 21). Amine solution was also added in or withdrawn periodically from the sample port to keep the liquid level constant in the wetted wall column.

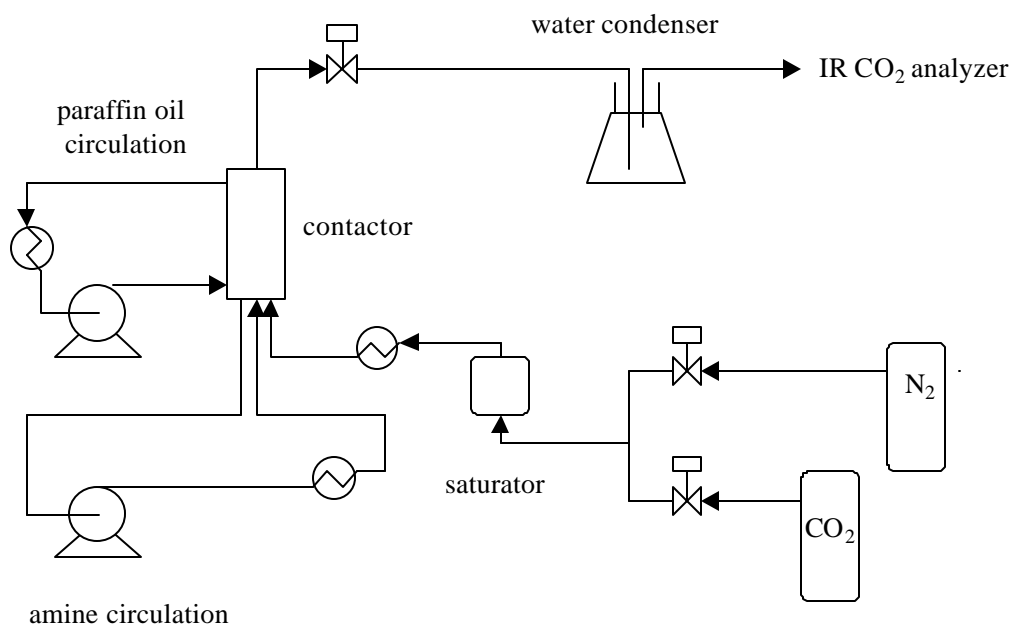


Figure 2. Overall experimental flowsheet.

### PHYSICAL PARAMETERS

Table 1 gives the methods for calculating physical parameters. The Henry's constant was calculated as a function of amine concentration, but not of CO<sub>2</sub> loading. The expressions for  $k_l^\circ$  and  $k_g$  were verified by previous investigators with CO<sub>2</sub> desorption from water and SO<sub>2</sub> absorption, respectively.

### DATA ANALYSIS AND EXPERIMENTAL RESULTS

In this work, at any given loading for a particular amine solution, both absorption and desorption rates were measured by variation of CO<sub>2</sub> partial pressure around the equilibrium partial pressure. When the flux is equal to zero, the partial pressure of CO<sub>2</sub> will be the equilibrium partial pressure of CO<sub>2</sub> at that loading. This point can be found by bracketing the absorption and desorption rates. Figure 3 gives an example of a 5.0 M MEA with 0.299 mol CO<sub>2</sub>/mol MEA. While inferring the equilibrium partial pressure, only measurements close to equilibrium were considered.

By applying the same method to every loading, we determined CO<sub>2</sub> equilibrium partial pressure at a number of solution compositions (table 2).

Table 1. Methods for Calculation of physical parameters.

Property	Formula	Comment
$\rho$ (g/cm <sup>3</sup> )	$\rho=(X_{Am}M_{AM}+X_{H2O}M_{H2O}+X_{CO2}M_{CO2})/V$	correction in V for solution nonideality (25)
$\mu$ (Pa-s)	$\mu/\mu_{H2O}=\exp\{[(a\Omega+b)T+(c\Omega+d)] [\alpha(e\Omega+fT+g)+1] \Omega/T^2\}$	(25)
H (atm/M)	$H_{CO2,MEA}=R*\exp[-2625/T+12.2]$ $R=\exp[(A/T+B)X_1]$	not a function of loading (17)
D (m <sup>2</sup> /s)	N <sub>2</sub> O analogy	Stokes-Einstein for D <sub>N2O,amine</sub> (24)
$k_l^o$ (cm/s)	$k_l^o=Q_L(1-\Theta)/a$	(22)
$k_g$ (mol/(Pa cm <sup>2</sup> /s))	$Sh=1.075(Re Sc d/h)^{0.85}$	(5)

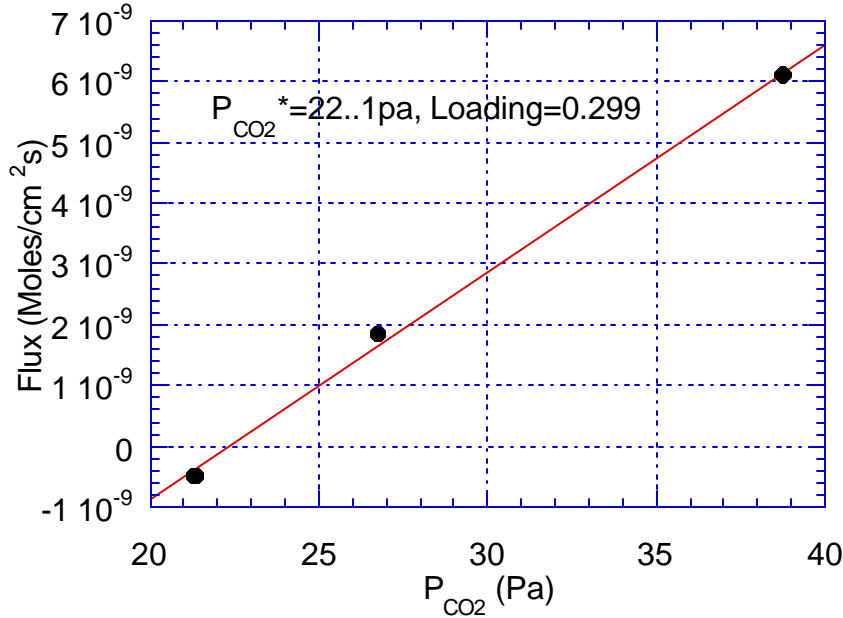


Figure 3. Extraction of CO<sub>2</sub> solubility in 5.0 M MEA at 40 °C, P<sub>CO2</sub>\*=22.1 Pa, 0.299 mol CO<sub>2</sub>/mol amine.

In the mass transfer process between the gas phase and the liquid phase, which is enhanced by chemical reactions, the total resistance to mass transfer was modeled as the sum of gas film (1/k<sub>g</sub>) and liquid film resistance (1/k<sub>G</sub>):

$$\frac{1}{k_g} + \frac{1}{k_G} = \frac{1}{K_G} \quad (1)$$

The total gas phase mass transfer coefficient, K<sub>G</sub>, was calculated by the following expression:

$$K_G = \frac{Flux}{P_{CO_2} - P_{CO_2}^*} \quad (2)$$

where,  $P_{CO_2}$  is the operational partial pressure of  $CO_2$  in the wetted wall column, which was calculated by the log mean average:

$$P_{CO_2} = \frac{P_{CO_2,in} - P_{CO_2,out}}{\ln\left(\frac{P_{CO_2,in}}{P_{CO_2,out}}\right)} \quad (3)$$

The liquid phase mass transfer coefficient with chemical reactions,  $k_G'$ , was calculated by where,  $P_{CO_2}^*$  is equilibrium partial pressure of  $CO_2$ , which is measured by bracketing both

$$k_G' = \frac{Flux}{(P_{CO_2,i} - P_{CO_2}^*)} \quad (4)$$

absorption and desorption data near equilibrium. The partial pressure of  $CO_2$  at the gas liquid interface,  $P_{CO_2,i}$ , is calculated by

$$P_{CO_2,i} = P_{CO_2} - \frac{Flux}{k_g} \quad (5)$$

$k_G'$  can also be expressed as:

$$\frac{1}{k_G'} = \frac{H}{k_i^o E} \quad (6)$$

where,  $E$  is the enhancement factor which is defined as the ratio of flux with chemical reactions to that without chemical reactions.

In table 2, six points have been identified that may have greater uncertainty. The uncertainty in the calculated value of  $E$  or  $k_G'$  is indicated by low values of the fraction removal of  $CO_2$ ,  $(P_{CO_2,i} - P_{CO_2,out})/P_{CO_2,in}$ , and the approach to equilibrium,  $(P_i - P^*)/P$ . Low removal of the  $CO_2$  (<20%) causes great uncertainty because the flux is determined as the difference between inlet and outlet concentrations. A small approach to equilibrium (<0.3) at the interface causes great uncertainty in the estimate of the driving force and includes the effect of a high gas film resistance. Estimates of  $P_{CO_2}^*$  are especially important with a small approach to equilibrium.

At each loading in a given amine concentration, the  $CO_2$  partial pressure was varied to obtain a series of rate data.  $CO_2$  flux is plotted versus liquid driving force ( $P_{CO_2,i} - P_{CO_2}^*$ ) to obtain a straight line.  $k_G'$  can be obtained from the slope of this straight line.  $E$  then is calculated from eq. 6. The measured rate data are summarized in table 2. The detailed data and error analysis are given in Dang (8).

Table 2. Measured and predicted enhancement factors for CO<sub>2</sub> absorption in MEA/PZ/H<sub>2</sub>O.

T (°C)	Amine(M)		Ldg	P <sub>CO<sub>2</sub>*</sub> (Pa)		**k <sub>G</sub> ' · 10 <sup>10</sup>	k <sub>l</sub> <sup>o</sup> (cm/s)	**E <sub>exp</sub>	E <sub>pred</sub>	E <sub>1</sub>	E <sub>inst</sub>	k <sub>G</sub> /k <sub>G</sub>	$\frac{P_{\text{exp}}}{P}$	Removal (%)
	MEA	PZ		exp	model									
60	0.4	0.6	0.057	18.2	1.5	4.70	0.016	174	136	137	21900	0.68	0.29*	42.4
			0.14	115	13	2.88	0.016	107	117	120	5090	0.54	0.26*	39
	2.5	0	0.091	27.6	4.6	3.18	0.015	120	98.4	98.7	38000	0.56	0.39	38.7
			0.33	254	300	1.54	0.015	58.5	72	73	4020	0.31	0.62	25
			0.614	7730	49000	0.54	0.015	20.4	16	28	38	0.19	0.25*	5.9*
	1.9	0.6	0.01	0.2	0.02	7.19	0.015	272	181	182	275000	0.73	0.27*	52.2
			0.21	102	56.4	3.14	0.014	127	144	145	12900	0.56	0.43	53.9
			0.44	2420	1500	1.46	0.013	64	74	87	480	0.39	0.31	31.1
	5.0	0	0.27	224	116	2.42	0.012	104	124	125	7310	0.48	0.42	32.5
			0.52	9550	20000	0.44	0.011	20.6	33	55	84	0.14	0.55	8.4*
	3.8	1.2	0.41	518	1003	2.96	0.011	140	172	183	2570	0.54	0.36	34.4
	40	5.0	0	0.30	22.1	29	2.00	0.0085	92	101	101	76800	0.43	0.51
0.47				768	852	0.42	0.0078	20.8	32	36	280	0.14	0.78	11.5*
3.8		1.2	0.43	90.5	118	2.04	0.0073	109	122	123	16600	0.44	0.35	24.3

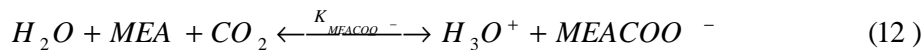
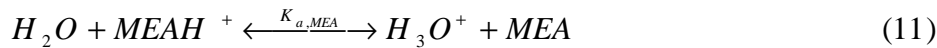
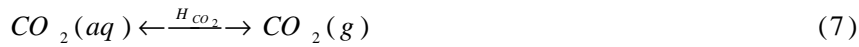
Ldg: loading (mol CO<sub>2</sub>/mol amine); k<sub>G</sub>' (mol/(cm<sup>2</sup>s-Pa)): normalized flux=flux/(P<sub>CO<sub>2</sub>,i</sub>-P<sub>CO<sub>2</sub>\*</sub>); k<sub>l</sub><sup>o</sup>: liquid phase mass transfer coefficient; E<sub>exp</sub>: measured enhancement factor; E<sub>pred</sub>: predicted enhancement factor; E<sub>1</sub>: predicted pseudo first order enhancement factor; E<sub>inst</sub>: instantaneous enhancement factor; exp: measured value; model: predicted value.

\* These parameter values are indicative of potential uncertainty in k<sub>G</sub>'

\*\* Values are calculated by using measured CO<sub>2</sub> equilibrium partial pressure, P<sub>CO<sub>2</sub>\*</sub>.

## SOLUBILITY AND SPECIATION MODEL

In the VLE model, one phase equilibrium and 5 chemical equilibria in the liquid phase were considered for CO<sub>2</sub>/MEA/H<sub>2</sub>O.



There are three material balance equations for CO<sub>2</sub>, MEA, and the whole solution respectively:

$$X_{CO_2,T} = X_{CO_2} + X_{HCO_3^-} + X_{CO_3^{2-}} + X_{MEACOO^-} \quad (13)$$

$$X_{MEA,T} = X_{MEA} + X_{MEA^H^+} + X_{MEACOO^-} \quad (14)$$

$$\sum X_i = 1 \quad (15)$$

Because the solution is neutral, there exists a charge balance:

$$0 = 2X_{CO_3^{2-}} + X_{HCO_3^-} + X_{OH^-} + X_{MEACOO^-} - X_{H_3O^+} - X_{MEA^H^+} \quad (16)$$

Assuming that the Henry's law constant and the equilibrium constants of the chemical reactions are available, the equilibrium partial pressure of CO<sub>2</sub> in the gas phase and the mole fractions of each species in the liquid phase can be calculated. However the literature values for the reaction equilibrium constants are for infinite dilution in water. In this work, the amine solution is concentrated and the strong ionic effects will change the system behavior. On one hand, this work uses the literature values of the water dissociation constant, CO<sub>2</sub> dissociation constant, and HCO<sub>3</sub><sup>-</sup> dissociation constant from Maurer (18) and Edwards et al. (10) respectively, and on the other hand, adjusts the pK<sub>a</sub> value of MEA (reaction (15)) and the carbamate stability constant of MEA (reaction (16)), to account for all of the nonideality of the system.

The solubility data of CO<sub>2</sub> in 5 M MEA at 60°C and 40°C of Jou et al. (12) were used to determine the two model parameters of the VLE model at 60°C and 40°C, respectively. The adjusted parameters are listed in table 3 and the literature values for the other equilibrium constants are listed in table 4. Because these equilibrium constants were defined in terms of mole fraction and activity coefficients, they are dimensionless. Figure 4 shows the result of the parameter fitting with the measured solubility data.

By introducing the following three chemical reactions, the VLE model was expanded to CO<sub>2</sub>/MEA/PZ with the equilibrium constants from Bishnoi et al. (5) listed in table 4.

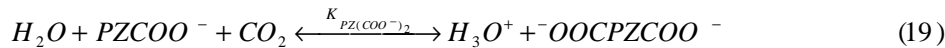
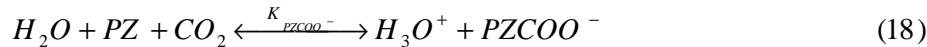
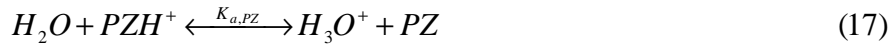


Table 3. Comparison of literature values to model parameters fitted to data from Jou (12).

	pK <sub>a</sub> (fitted)	pK <sub>a</sub> (3)	K <sub>MEACOO<sup>-</sup></sub> (fitted)	K <sub>MEACOO<sup>-</sup></sub> (2)
5.0 M MEA, 60°C	9.18E-12	1.45E-11	5.84E-6	2.87E-5
5.0 M MEA, 40°C	1.26E-12	3.51E-12	5.03E-6	5.51E-5

Table 4. Temperature dependence of the equilibrium constants.

$$\ln K = C_1 + C_2/T(K) + C_3 \ln T(K)$$

reaction	C <sub>1</sub>	C <sub>2</sub>	C <sub>3</sub>	Source
K <sub>H2O</sub>	132.899	-13445.9	-22.4773	Maurer (18)
K <sub>a,CO2</sub>	231.465	-12092.1	-36.7816	Edwards et al. (10)
K <sub>a,HCO3<sup>-</sup></sub>	216.049	-12431.7	-35.4819	Edwards et al. (10)
K <sub>a,PZ</sub>	-11.91	-4350.6	0	Bishnoi et al. (4)
K <sub>PZCOO<sup>-</sup></sub>	-29.308	5614.64	0	Bishnoi et al. (4)
K <sub>PZ(COO<sup>-</sup>)<sub>2</sub></sub>	-30.777	5614.64	0	Bishnoi et al. (4)

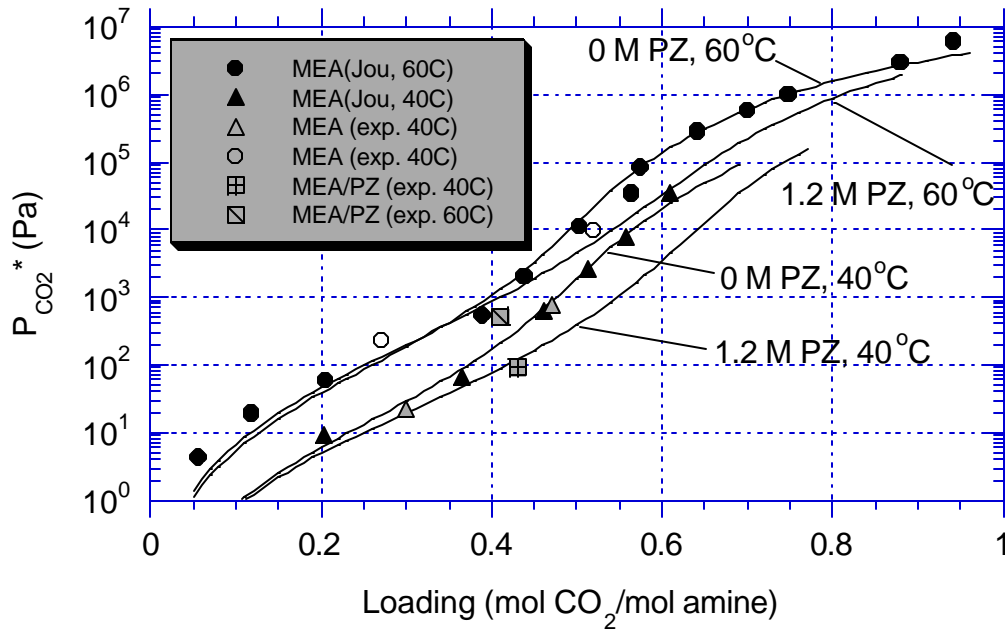


Figure 4. CO<sub>2</sub> solubility in 5 M amine (MEA+PZ) at 60°C and 40°C, predicted by parameters in table 2.3, data from Jou (12).

The predicted speciation of CO<sub>2</sub> in 1.9 M MEA/0.6 M PZ at 60°C, and in 3.8 M MEA/1.2 M PZ by this model is shown in figures 5 and 6.

Figure 7 shows the predicted solubility by the VLE model with the literature data and the measured solubility of this work for CO<sub>2</sub> absorption in 5.0 M MEA at 40 and 60°C. At 40°C, the data from this work, model prediction, and literature match each other very well. At 60°C, experimental data matches the available literature data well, but the experimental data only fits the model prediction well at medium loading. The discrepancy might be because that the model itself does not fit the literature data well, which was used to fit the model parameters. At low or high loading, for example, the error may be more than 100%

In figure 7, both calculated curves and measured data indicate that the addition of PZ to MEA can decrease the CO<sub>2</sub> equilibrium partial pressure by a factor of 2-5 at medium and high loading, but has no significant effect at low loading.



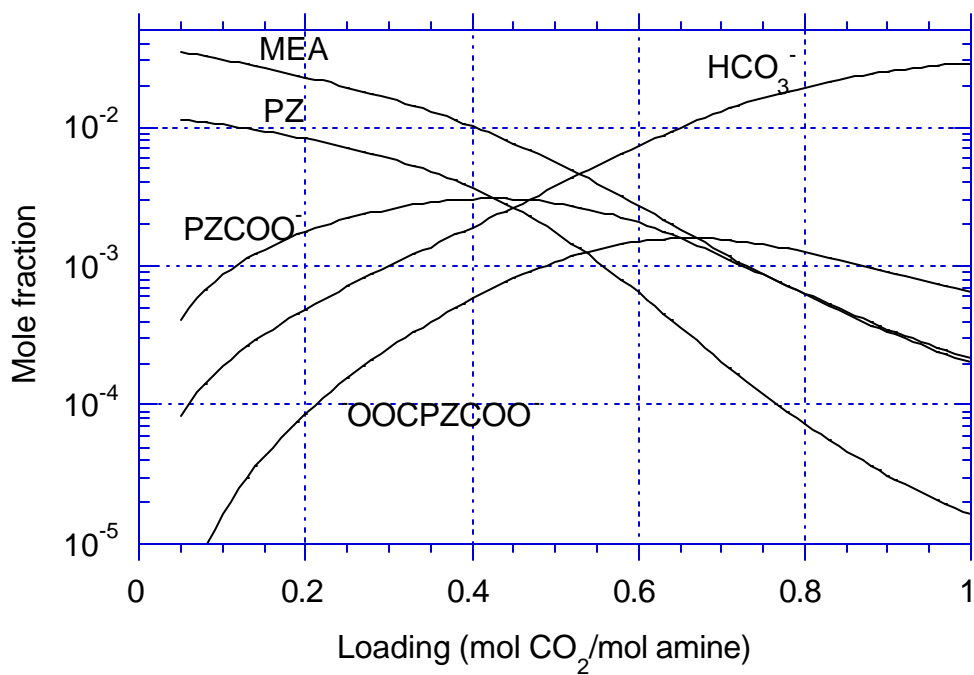


Figure 5. Predicted speciation of CO<sub>2</sub> in 1.9 M MEA/0.6 M PZ at 60°C.

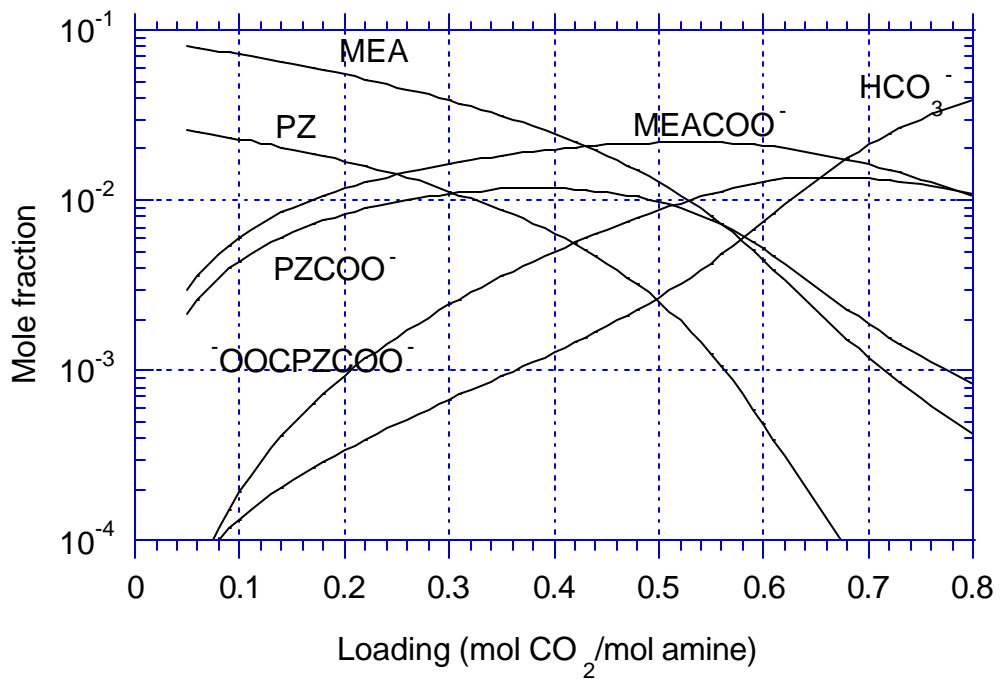


Figure 6. Predicted speciation of CO<sub>2</sub> in 3.8 M MEA/1.2 M PZ at 40°C.

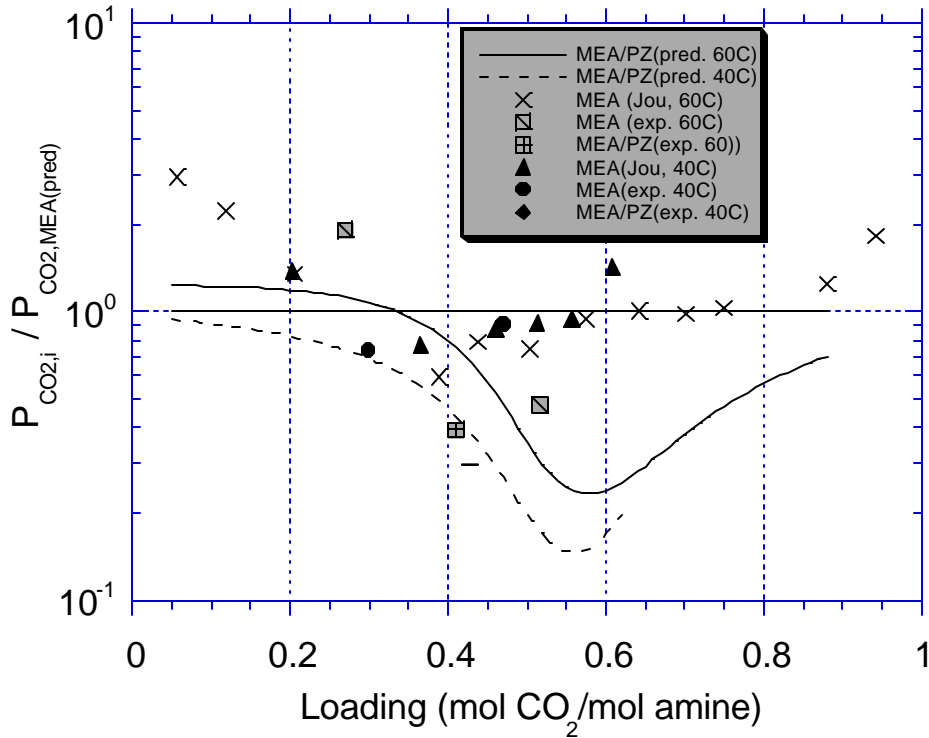


Figure 7. Comparison of predicted CO<sub>2</sub> solubility, literature data, and experimental data in 5.0 M MEA blends with 0 or 1.2 M PZ at 60°C and 40°C.

### RATE MODEL

This work uses a simple rate model to predict the enhancement factor  $E$  for CO<sub>2</sub> absorption in MEA/PZ/H<sub>2</sub>O. The model includes two contributions: pseudo first order enhancement and instantaneous enhancement.

#### Pseudo First Order Enhancement Factor

In the CO<sub>2</sub>/MEA/PZ/H<sub>2</sub>O system, three finite-rate, reversible reactions, 12, 18, and 19 are important. If the MEA, PZ and PZCOO<sup>-</sup> concentration gradients in the liquid film are neglected and represented by their bulk values respectively, the analytical expression for the pseudo-first order enhancement factor,  $E_1$ , can be derived by shell balance:

$$E_1 = \frac{\sqrt{(k_{MEA}[MEA] + k_{PZ}[PZ] + k_{PZCOO^-}[PZCOO^-])D_{CO_2}}}{k_1^o} \quad (20)$$

With the assumption of pseudo first order, [MEA], [PZ], and [PZCOO<sup>-</sup>] are the concentrations of these species in the bulk solution.  $k_{MEA}$ ,  $k_{PZ}$ , and  $k_{PZCOO^-}$  are the second order rate constants of MEA, PZ, and PZCOO<sup>-</sup> with CO<sub>2</sub> respectively.  $k_{MEA}$  and  $k_{PZ}$  were calculated by equations 21 (11) and 22 (5).  $k_{PZCOO^-}$  was assumed to be one fourth of  $k_{PZ}$ .

$$\text{Log}_{10}(0.001 * k_{MEA} (m^3 / mole \cdot s)) = 10.99 - 2152 / T(K) \quad (21)$$

$$k_{pZ}(m^3 / mol \cdot s) = 0.001 * k_{25^\circ C} \exp\left[\frac{-\Delta H_a}{R} \left(\frac{1}{T(K)} - \frac{1}{298}\right)\right] \quad (22)$$

where,  $k_{25^\circ C} = 5.37E4 \text{ m}^3/\text{kmol}$ ,  $\Delta H_a = 3.36E4 \text{ kJ/kmol}$ . In this work, the liquid film mass transfer coefficient,  $k_l^\circ$ , varies from  $0.8E-4$  to  $1.6E-4 \text{ m/s}$ .

### Instantaneous Enhancement Factor

To account for the effect of the diffusion of reactants and products on the mass transfer process, the simple model includes an estimation of the instantaneous enhancement factor,  $E_{inst}$ :

$$E_{inst} = C_{amine} H_{CO_2} \frac{\Delta(\text{loading})}{\Delta(P_{CO_2}^*)} \sqrt{\frac{D_{CO_2}}{D_{product}}} \quad (23)$$

If the flux is small and  $P_{CO_2}^*$  across the interface is small, equation 27 reduces to:

$$E_{inst} = C_{amine} H_{CO_2} \frac{\partial(\text{loading})}{\partial(P_{CO_2}^*)} \sqrt{\frac{D_{CO_2}}{D_{product}}} \quad (24)$$

The derivative of the equilibrium loading with equilibrium partial pressure was determined numerically from the results of the VLE model. This means  $E_{inst}$  is a global instantaneous enhancement factor which assumes that the reactions of MEA, PZ, and PZCOO<sup>-</sup> with CO<sub>2</sub> are all instantaneous. The ratio of  $D_{CO_2}$  to  $D_{product}$  was approximated by a value of 2.0.

### Total Enhancement Factor

The simple model is completed by assuming a series resistance. If the reaction occurs near the interface, then reaction enhancement  $E_1$  is in series with instantaneous enhancement  $E_{inst}$ .

Equation 25 can also be derived by combining equations 26, 27, and 28:

$$\frac{1}{E} = \frac{1}{E_1} + \frac{1}{E_{inst}} \quad (25)$$

$$\text{flux} = E_1 ([CO_2]_i - [CO_2]_i^*) k_l^\circ \quad (26)$$

$$\text{flux} = E_{inst} ([CO_2]_i^* - [CO_2]_b^*) k_l^\circ \quad (27)$$

$$\text{flux} = E ([CO_2]_i - [CO_2]_b^*) k_l^\circ \quad (28)$$

## RESULTS

Table 2 and figures 8-10 compare the measured and calculated CO<sub>2</sub> absorption rate. The predictions agree well with the measured data at medium loading in 1.0 M MEA/PZ and 2.5 M MEA/PZ, but overestimate the rate for 5.0 M MEA/PZ at both 40 and 60°C.

Both the calculated and the measured data show that 0.6 M PZ in 1.0 M MEA increases the rate by a factor of 2 to 2.5 at 60°C. The addition of 0.6 M PZ to 2.5 M MEA and 1.2 M PZ to 3.8 M MEA increase the rate by a factor of 1.5 to 2 at 40 and 60°C.

The relative effect of PZ ( $E_{\text{MEA/PZ}}/E_{\text{MEA}}$ ) is practically independent of  $\text{CO}_2$  loading, except at very high loading. This is because  $\text{PZCOO}^-$  is also a reactive species with  $\text{CO}_2$ . Only at very high loading (0.8-0.9), are both PZ and  $\text{PZCOO}^-$  depleted.

In both MEA/PZ and MEA solvents, when the loading of lean solutions increases to 0.5 mol  $\text{CO}_2$ /mol amine, the enhancement factors decrease by a factor of 2 to 3. This is because of the consumption of the reactive species with loading.

The simple rate model (figures 9 and 10) indicates that at higher temperature, both MEA and MEA/PZ have higher rates than at lower temperature. There is no significant difference in the relative effect of PZ ( $E_{\text{MEA/PZ}}/E_{\text{MEA}}$ ) between 40 and 60°C.

### **Rate Contributions of Important Species**

The speciation of the amine solution plays a very important role in the  $\text{CO}_2$  absorption rate. The contributions of three important species in MEA/PZ blends, (MEA, PZ, and  $\text{PZCOO}^-$ ), to the total absorption rate are compared in figure 11. The rate fraction of each species is calculated as:

$$\text{rate fraction of species } i = k_i[i]/(k_{\text{MEA}}[\text{MEA}] + k_{\text{PZ}}[\text{PZ}] + k_{\text{PZCOO}^-}[\text{PZCOO}^-]) \quad (29)$$

where,  $k_i$  is the rate constant of species  $i$  (MEA, PZ, and  $\text{PZCOO}^-$ ) with  $\text{CO}_2$  as given by equations 21 and 22.  $K_{\text{PZCOO}^-}$  is assumed to be 25% of  $k_{\text{PZ}}$ .  $[i]$  is the concentration of each species calculated by the VLE model of this work.

Figure 11 shows the rate fractions of MEA, PZ, and  $\text{PZCOO}^-$  in 3.8 M MEA/1.2 M PZ at 60°C. At loading less than 0.5, PZ contributes more than 50% of the total absorption rate. When the loading is higher than 0.65,  $\text{PZCOO}^-$  contributes more than 50% of the total reaction rate. MEA contributes 20-30% of the rate throughout the range of loading.

The contribution of  $\text{PZCOO}^-$  is only important at high loading because we have assumed that  $k_{\text{PZCOO}^-} = 0.25 k_{\text{PZ}}$ . We saw little effect of  $k_{\text{PZCOO}^-}$  when it was reduced to 10% of  $k_{\text{PZ}}$  (8). In modeling of data for MDEA/PZ, Bishnoi (6) used  $k_{\text{PZCOO}^-} \approx k_{\text{PZ}}$ . However, there was still a large uncertainty in the estimate of  $k_{\text{PZCOO}^-}$ .

### **Effect of Reactant and Product Diffusion**

The pseudo-first order enhancement factor accounts for the effect of chemical reactions on the  $\text{CO}_2$  absorption rate, but it does not account for reactant depletion or product accumulation at the gas-liquid interface. In figure 8, the two types of dashed lines show the significance of the pseudo first order and instantaneous contributions to the enhancement factor. With loading less than 0.5 mol  $\text{CO}_2$ /mol amine, the pseudo first order model represents the overall enhancement accurately. At higher loading, instantaneous enhancement becomes important and even dominant. The instantaneous enhancement factor in MEA and MEA/PZ is almost identical, therefore, the difference in kinetics accounts for the promotion of  $\text{CO}_2$  absorption by PZ in MEA solution.

### **Amine Depletion at the Gas-Liquid Interface**

In this paper, the rate model combines as series resistances the estimated values of the pseudo first order and instantaneous enhancement factor. The estimation of the instantaneous enhancement factor assumes that there is a low driving force and flux. The combination of the resistances assumes that there is no depletion of amine at the gas-liquid interface. Neither of

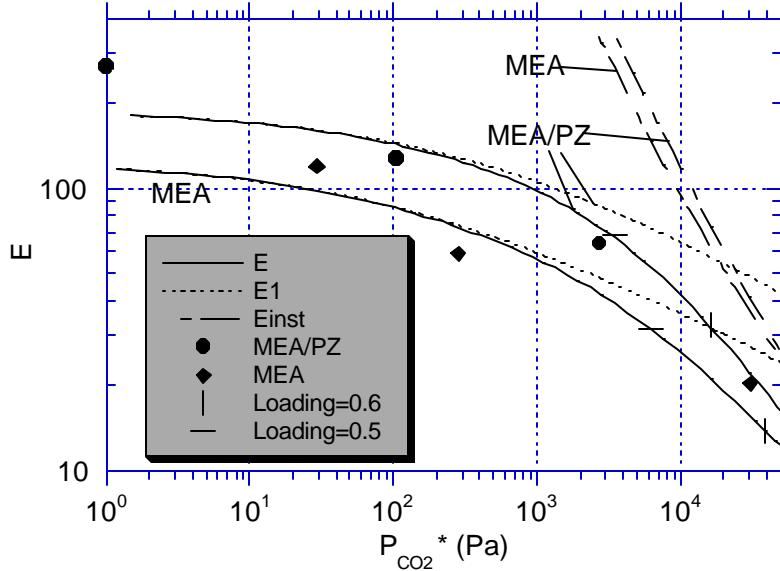


Figure 8. CO<sub>2</sub> absorption rate in 2.5 M amine with 0 or 0.6M PZ at 60°C, curves predicted by the rate model with the listed constants.  $D_{CO_2}=4.11E-5$  cm<sup>2</sup>/s,  $k_{MEA}=3.37E4$  L/mol-s,  $k_{PZ}=2.23E5$  L/mol-s,  $k_{PZCOO^-}=5.58E4$  L/mol-s,  $k_1^0=0.015$  cm/s.

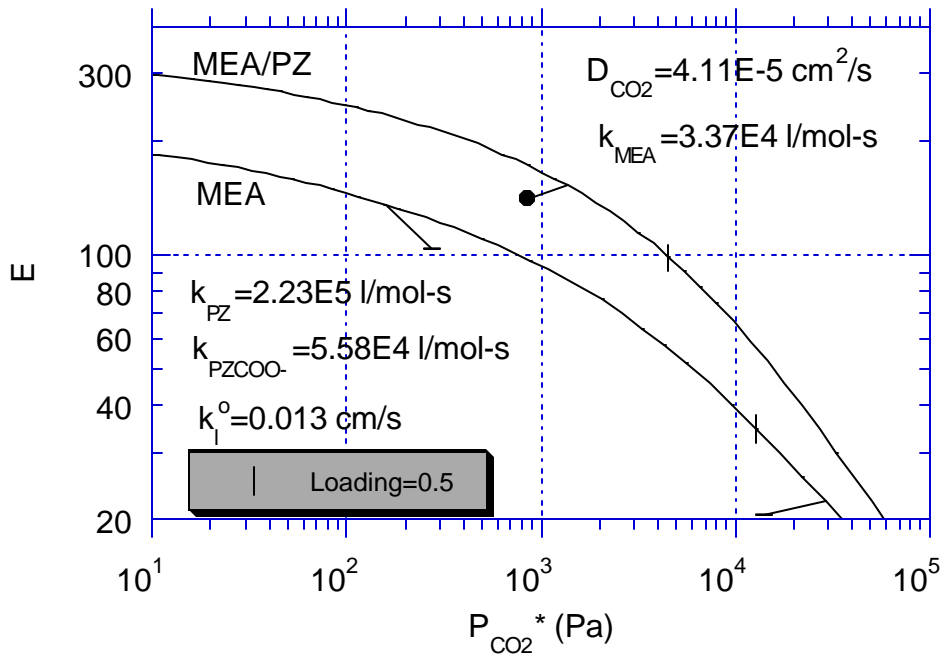


Figure 9. CO<sub>2</sub> absorption rate in 5.0 M amine with 0 or 1.2 M PZ at 60°C, curves predicted by the rate model with the listed constants, line segments connect values of equal loading.

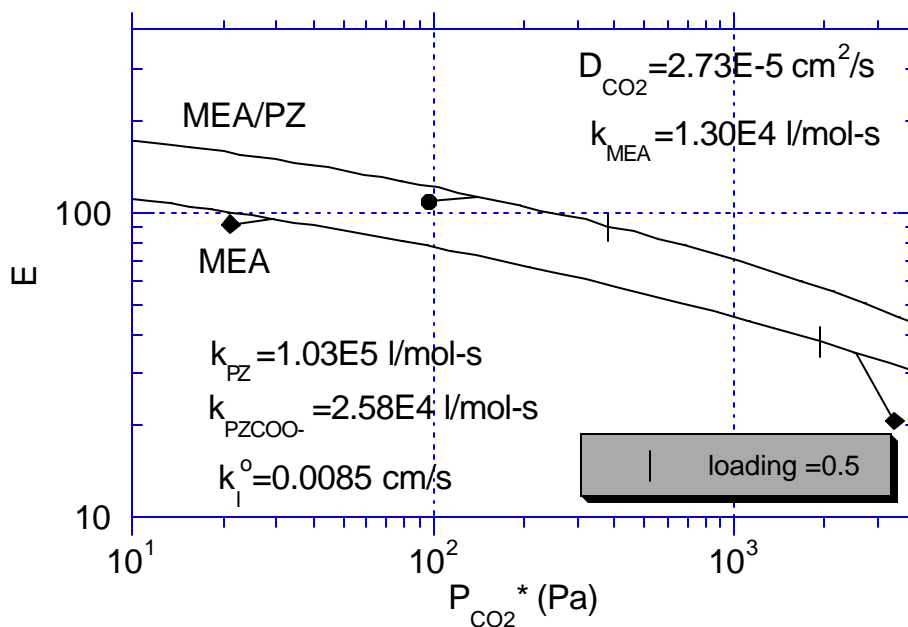


Figure 10. CO<sub>2</sub> absorption rate in 5.0 M amine with 0 or 1.2 M PZ at 40°C, curves predicted by the rate model with the listed constants, line segments connect values of equal loading.

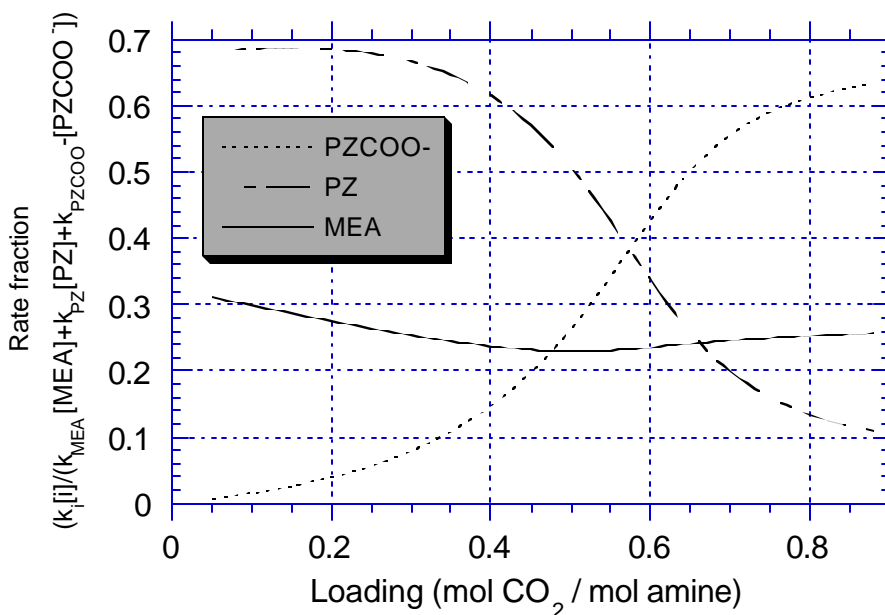


Figure 11. Contributions of reactive amine species to the CO<sub>2</sub> reaction rate in 3.8 M MEA/1.2 M PZ at 60°C.

these assumptions is good with the measurements at high loading, usually made with a large driving force and a large flux. Therefore, a more rigorous model would be more accurate in predicting the enhancement at high loading.

## CONCLUSIONS

The absorption rate of CO<sub>2</sub> at 40 and 60°C in aqueous MEA with 0.6 to 1.2 M PZ is 1.5-2.5 times greater than that in MEA alone.

In both MEA and MEA/PZ solvents, the CO<sub>2</sub> enhancement factor is 2 to 3 times smaller in rich solutions (0.5 mol CO<sub>2</sub>/mol amine) than in lean solutions. Therefore, a larger fraction of the absorber packing height will be devoted to mass transfer under rich conditions. This effect results from the depletion of MEA and PZ at greater loading.

With less than 0.4 mol CO<sub>2</sub>/mol amine, the PZ species contributes more than 60% of the total absorption rate. With loading more than 0.6 mol CO<sub>2</sub>/mol amine, the species PZCOO<sup>-</sup> accounts for more than 40% of total absorption rate. For most of the cases studied in this work, MEA has a 20% to 30% contribution to the total absorption rate over the whole range of loading.

At 40 and 60°C, and loading greater than 0.4 to 0.5 mol CO<sub>2</sub>/mol amine, the equilibrium partial pressure of CO<sub>2</sub> in aqueous MEA with 0.6 to 1.2 M PZ is 2 to 5 times smaller than with MEA alone. At loading less than 0.2 to 0.3, there is no significant effect of PZ on the equilibrium partial pressure of CO<sub>2</sub>.

The effects of PZ, CO<sub>2</sub> loading, and temperature are predicted well by the simple model combining estimated values of the pseudo first order and instantaneous enhancement factors. This simple model predicts accurate values of the enhancement factors in 1.0 and 2.5 M amine, but overpredicts the enhancement in 5.0 M amine by 10 to 80%. A more rigorous simulation of reactant and product diffusion may be necessary at these conditions.

## NOMENCLATURE

d	hydraulic diameter of the wetted wall column (m)
D	diffusion coefficient (m <sup>2</sup> /s)
E	enhancement factor
h	height of the wetted wall column (m)
H	Henry's law constant (Pa <sup>-1</sup> )
I	ionic strength
k	rate constant (m <sup>3</sup> /mol s)
k <sub>g</sub>	gas film mass transfer coefficient (mol/(Pa·cm <sup>2</sup> ·s))
k <sub>G</sub>	mass transfer coefficient based on gas phase (mol/(Pa·cm <sup>2</sup> ·s))
k <sub>l</sub> <sup>o</sup>	liquid film mass transfer coefficient (m/s)
K	equilibrium constant
M	molecular weight
P <sub>x</sub>	partial pressure of x (Pa)
Q <sub>L</sub>	flow rate (m <sup>3</sup> /s)
Re	Reynolds number
Sc	Schmidt number
Sh	Sherwood number

T	temperature (K)
V	volume of solution (m <sup>3</sup> )
X	mole fraction
$\alpha$	CO <sub>2</sub> loading (mol CO <sub>2</sub> /mol amine)
$\Theta$	parameter to calculate mass transfer coefficient
$\mu$	viscosity (Pa·s)
$\rho$	density (kg/m <sup>3</sup> )
	mass percent of amine

## REFERENCES

1. G. Astarita, *Chem. Eng. Sci.*, 16, 202 (1961).
2. M. D. Austgen, G. T. Rochelle, "Model of Vapor-Liquid Equilibrium for Aqueous Acid Gas-Alkanolamine System Using Electrolyte-NRTL Equation", *Amer. Chem. Soc.*, 28, 1060 (1989).
3. R. G. Bates, G. D. Pinching, "Acidic Dissociation Constant and Representation and Prediction of Deviation from Ideality in Electrolyte Solutions Compared to the Models of Chen (1982) and Pitzer (1973)", *AIChE J.* 31(3), 392 (1985).
4. S. Bishnoi, "Physical and Chemical Solubility of Carbon Dioxide in Aqueous Methyl-diethanolamine", M.S. Thesis, The University of Texas at Austin, December, (1998).
5. S. Bishnoi, G. T. Rochelle, "Absorption of Carbon Dioxide into Aqueous Piperazine: Reaction Kinetics, Mass Transfer and Solubility", *Chem. Eng. Science*, 55, 5531 (2000).
6. S. Bishnoi, "Carbon Dioxide Absorption and Solution Equilibrium in Piperazine Activated Methyl-diethanolamine", Ph.D Dissertation, The University of Texas at Austin, December, (2000).
7. P. V. Danckwerts, M. M. Sharma, *Chem. Eng.*, 10, 244 (1966).
8. H-Y. Dang, "Carbon Dioxide Absorption Rate and Solubility in Monoethanolamine/Piperazine/Water", M.S. Thesis, The University of Texas at Austin, May, (2001).
9. T. L. Donaldson, Y. N. Nguyen, *Ind. Eng. Chem. Fund.*, 19, 260 (1980).
10. T. J. Edwards, G. Mauer, J. Newman, J. M. Prausnitz, "Vapor-Liquid Equilibria in Multicomponent Aqueous Solution of Volatile Weak Electrolytes", *AIChE J.*, 24(6), 996 (1978).
11. H. Hikita, S. Asai, H. Ishikawa, M. Honda, "The Kinetics of Reactions of Carbon Dioxide with Monoethanolamine, Diethanolamine and Triethanolamine by a Rapid Mixing Method", *Chem. Eng. J.*, 13, 7 (1977).
12. F-Y Jou, A. E. Mather, F. D. Otto, "The Solubility of CO<sub>2</sub> in a 30 Mass Percent Monoethanolamine Solution", *Can. J. Chem. Eng.*, 73, 140 (1995).
13. S. Kaganoi, "Carbon Dioxide Absorption in Methyl-diethanolamine with Piperazine or Diethanolamine: Thermodynamics and Rate Measurements", M.S. Thesis, The University of Texas at Austin, (1997).
14. S. S. Laddha, P. V. Danckwerts, *Chem. Eng. Sci.*, 36, 479 (1981).
15. J. I. Lee, F. D. Otto, A. E. Mather, "Equilibrium Between Carbon Dioxide and Aqueous Monoethanolamine Solutions", *Appl. Chem. Biotechnol.*, 26, 541 (1976).
16. J. I. Lee, F. D. Otto, A. E. Mather, "The Solubility of H<sub>2</sub>S and CO<sub>2</sub> in Aqueous Monoethanolamine Solutions", *Can. J. Chem. Eng.*, 52, 803 (1974).



17. S. E. Licht, R. H. Weiland, "Density and Physical Solubility of Carbon Dioxide in Partial-Loaded Solution of MEA, DEA, and MDEA and Their Blends", Presented at the Spring National Meeting, American Institute of Chemical Engineers, Houston, Texas, April 2-6, (1989).
18. G. Maurer, "On the Solubility of Volatile Weak Electrolytes in Aqueous Solutions. In Thermodynamics of Aqueous Systems with Industrial Applications; Newman, S. A., Ed.,; ACS Symp. Ser. 133; American Chemical Society: Washington, DC, pp 139-186 (1980).
19. M. Mshewa, G. T. Rochelle, "Carbon Dioxide Desorption/Absorption with Aqueous Mixture of Methyldiethanolamine and Diethanolamine at 40°C to 120°C". Ph.D Dissertation, The University of Texas at Austin, (1995).
20. M. A. Pacheco, "Mass Transfer, Kinetics and Rate-Based Modeling of Reactive Absorption", Ph.D Dissertation, The University of Texas at Austin, (1998).
21. M. A. Pacheco, S. Kaganoi, G. T. Rochelle, "CO<sub>2</sub> Absorption into Aqueous Mixtures of Diglycolamine® and Methyldiethanolamine", *Chem. Eng. Sci.*, 55, 5125 (2000).
22. R. L. Pigford, "Counter-Diffusion in a Wetted Wall Column", Ph.D Dissertation, The University of Illinois, Urbana, Illinois, (1941).
23. K-P. Shen, M-H. Li, "Solubility of Carbon Dioxide in Aqueous Mixtures of Monoethanolamine with Methyldiethanolamine", *J. Chem. Data.*, 37, 96 (1992).
24. G. F. Versteeg, W. P. M. van Swaaij, "Solubility and Diffusivity of Acid Gas (CO<sub>2</sub>, N<sub>2</sub>O) in Aqueous Alkanolamine Solutions", *J. Chem Eng. Data.*, 33, 29 (1988).
25. R. H. Weiland, J. C. Dingman, D. B. Cronin, G. J. Browning, "Density and Viscosity of Some Partial Carbonated Aqueous Alkanolamine Solutions and Their Blends", *J. Chem. Eng. Data.*, 43, 378 (1998).
26. G-W. Xu, C-F. Zhang, S-J. Qin, W-H. Gao, H-B. Liu, "Gas-Liquid Equilibrium in CO<sub>2</sub>-MDEA-H<sub>2</sub>O System and the Effect of Piperazine on It", *Ind. Eng. Chem. Res.*, 37, 1473-1477 (1998).
27. G-W. Xu, C-F. Zhang, S-J. Qin, Y-W. Wang, "Kinetics Study on Absorption of Carbon Dioxide into Solutions of Activated Methyldiethanolamine", *Ind. Eng. Chem. Res.*, 31, 921-927 (1992).
28. G-W. Xu, C-F. Zhang, S-J. Qin, B-C. Zhu, "Desorption of CO<sub>2</sub> from MDEA and Activated MDEA Solution", *Ind. Eng. Chem. Res.*, 34, 874-880 (1995).